Journal of Crystal Growth 134 (1993) 281–286
North-Holland

JOURNAL OF CRYSTAL GROWTH

Infrared contrast of inclusions in CdTe

H.G. Brion, C. Mewes, I. Hahn and U. Schäufele

Kristall-Labor, Institut für Metallphysik, Universität Göttingen, Hospitalstrasse 12, D-37073 Göttingen, Germany

Received 7 April 1993; manuscript received in final form 28 July 1993

CdTe crystals have been grown by the Bridgman method with excess Cd and Te. Transmission infrared (IR) microscopy revealed inclusions in the monocrystalline CdTe matrix. Energy dispersive X-ray (EDX) analysis has been performed to determine their composition. Cd inclusions show a very specific contrast in the IR microscope. This contrast is discussed in terms of dislocations due to stress relief on account of a volume misfit between a Cd inclusion and the CdTe matrix.

1. Introduction

CdTe is very promising material for nuclear detectors, electro-optical modulators and optical devices in the infrared region. However, many of the applications of CdTe are still very limited, because of the lack of high quality, large bulk single crystals. CdTe substrates exhibit crystalline defects such as grains, sub-grains, twins, dislocations and inclusions. The formation of the latter depend on the stoichiometry of the compound and the crystal growth process including the subsequent cooling [1–4]. Tellurium as well as Cd inclusions are observed [4–6]. Their distribution is affected by the crystalline defect structure of the ingot. The surface, grain and twin boundaries are favourable sites for the formation of inclusions [6,7]. Due to the poor crystalline quality a very inhomogenous distribution is generally observed. Therefore little is known about the precipitation kinetics.

In this paper we have analysed by EDX inclusions of crystals grown from different melt compositions. We report a profound difference in infrared image contrast between Cd and Te inclusions.

2. Experimental procedure

CdTe crystals have been grown by the Bridgman method in sealed quartz ampoules coated with graphite. To keep the melt composition constant, an additional Cd reservoir (0.5–1.0 g) in the upper part of the ampoule was maintained at a fixed temperature during the crystal growth process (760–890°C corresponding to a Cd partial pressure of 1–2.8 Pa). A three-zone furnace was used similar to the one described by Triboulet and Marfaing [9]. Firstly, CdTe was synthesized from the elements Cd and Te (99.9999) supplied by Cominco. This presynthesized CdTe (total weight 100 g) was used for crystal growth in a second ampoule. The ingots had a diameter of 1.5 cm and a length of 10 cm. They contain single crystals about 2–3 cm^3 in size, some of them permeated by twin lamellae. A few crystal growth experiments were performed with excess Te (up to 10 g in the melt).

The specimens were obtained either by cleavage along {110} planes or cut with a wire saw.The surfaces were lapped with boron carbide and afterwards with diamond spray (down to 1 μm). No chemical polishing was performed, to avoid variations in composition in the surface area.

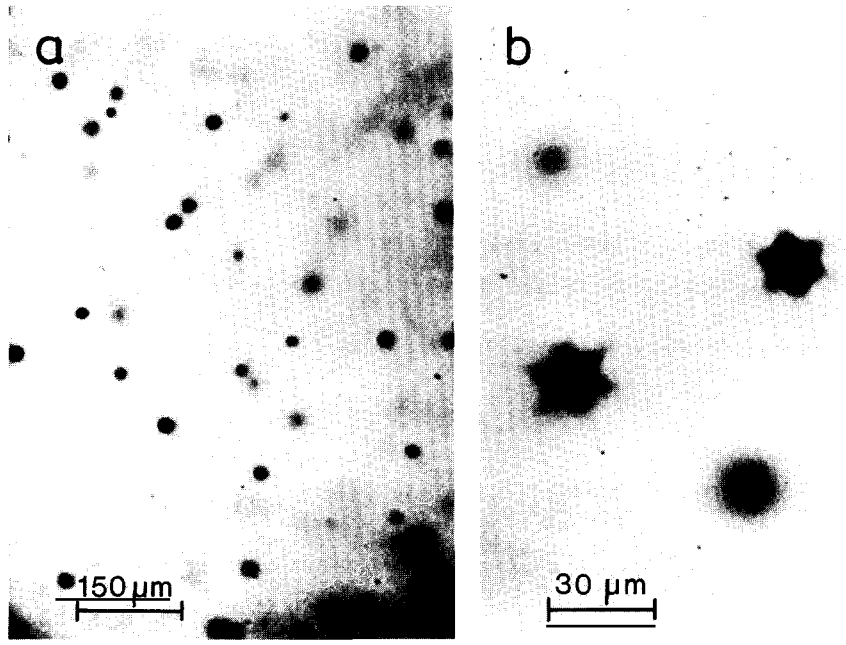

Fig. 1. (a) IR microscope image showing in an overview the distribution of inclusions in a crystal grown with excess Cd (reservoir temperature 890°C). (b) IR contrast of a few inclusions at higher magnification.

For SEM/EDX investigations, a Cambridge S 360 scanning electron miroscope was used fitted with an EDX spectrometer AN 10000 by Link. The IR micrographs were taken in a Zeiss light microscope Axiotron supplied with a Hamamatsu IR Vidicon C 2400-03. The camera had an imaging tube sensitive to 1.8 μm.

3. Results

In fig. 1a, an IR microscope image taken from the central part of a single crystalline specimen shows the general appearance of the inclusion distribution. The Cd reservoir temperature was 890°C. The circular dots represent the inclusions. Higher magnification reveals a six-pointed star (fig. 1b) of approximately 20–30 μm in diameter. The contrast size depends on the intensity of the illumination. With high intensity the contrast shrinks, whereas with a lower one it expands. Recently, a similar contrast was observed by Watson et al. [5].

To analyse the chemical composition of the inclusion by EDX, one has to bring up a single inclusion from the depth of the volume on top of the surface by subsequent removal of surface layers. This was achieved by mechanical polishing until the inclusions were sectionated as shown in fig. 2. In figs. 3a and 3b, the EDX spectra taken from the matrix and the inclusion are shown,

Fig. 2. SEM photograph of an inclusion cut by the surface (excess Cd).

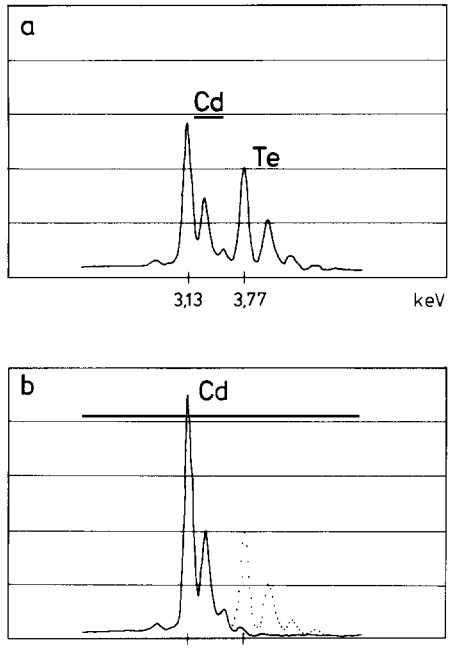

Fig. 3. EDX spectra taken from the matrix (a) and the inclusion (b) in fig. 2. The dotted Te peak has disappeared.

indicating that the inclusion contains much more Cd than Te.

The real size of the inclusion can be estimated in the following way. In fig. 4 several inclusions of different size and position are drawn schematically having the same intersection plane with the specimen surface. For the inclusion with a diameter of 4 μm this section plane coincides with its sagittal plane. Then the circle diameter corresponds directly with the one of the inclusion. For all other cases the centre of the inclusion is either above or below the surface. The EDX analysis was performed with an acceleration voltage of 20 kV. According to Kanaya and Okayama [9], the penetration depth for electrons in CdTe is 2.6 μm. For the excitation of the characteristic radiation, an interaction depth of 1 μm can be estimated. Twice the excitation energy is assumed to be needed for a sufficient quantum efficiency.

As shown in fig. 4, the transition in chemical composition matrix/inclusion is not sharp for larger diameters. Within a depth of 1 μm, Cd (hatched) and CdTe are excited simultaneously in the transition area. In our EDX analysis the Te peak vanished completely within the inclusion on a length of 1 μm from the phase boundary. This corresponds to an uncertainty in diameter of the same order. Thus the real diameter of the investigated inclusion can be limitated between 4 and 5 μm.

We investigated crystals grown with reservoir temperatures ranging from 760°C up to 890°C. Below 800°C and a maximum magnification of 500, no inclusion contrast could be detected in the IR microscope. At 820°C many small contrasts of 10 μm in diameter with a few of 30 μm in diameter were visible. With increasing reservoir temperature the volume fraction of the larger particles increases. A systematic variation of the inclusion diameter or in the volume fraction dependence with reservoir temperature could not be obtained. Due to the structural imperfections, some of the excess component preferentially diffuses to the grain and twin boundaries and to the surface.This results in a very inhomogeneous particle distribution. Within the temperature range 800–820°C, the medium contrast size is 10 μm in diameter and less. These inclusions appear spherical and a star-shaped structure could not be resolved anymore.

Some crystals grown with excess Te were investigated, too. The overview in fig. 5a looks very similar to the one in fig. 1a. In contrast to the Cd precipitates, the size does not change with the intensity of illumination. In focus with higher magnification (fig. 5b), the inclusions are very

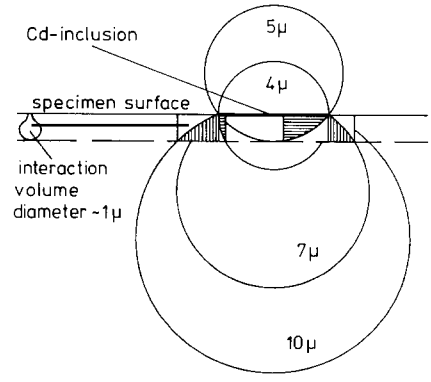

Fig. 4. Schematic drawing of spherical inclusions of different diameter having the same section plane with the surface.

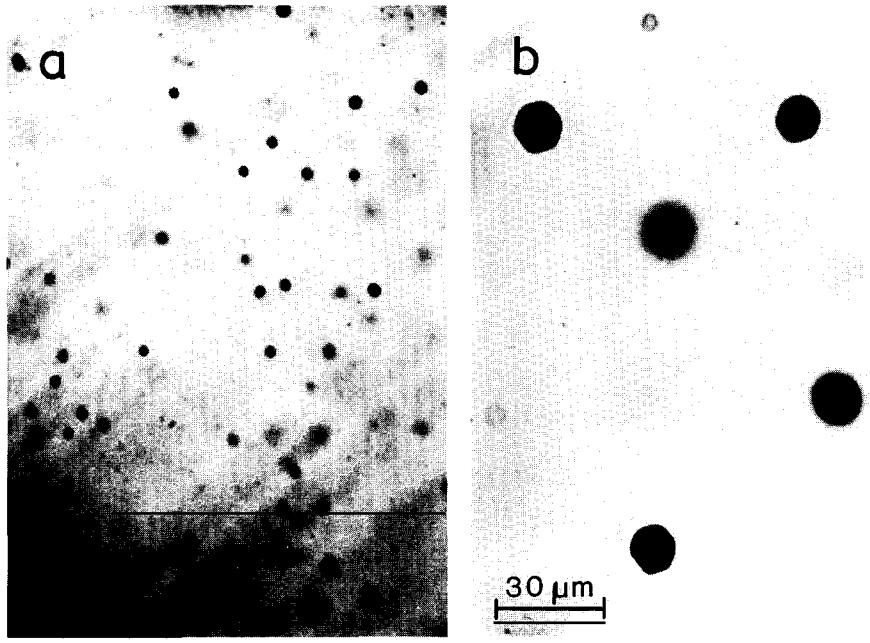

Fig. 5. (a) IR microscope image showing in an overview the distribution of inclusions in a crystal grown with excess Te. (b) IR contrast of a few inclusions with higher magnification.

uniform black with a sharp rim. For bigger inclusions the circular curvature deteriorates to secants. This can occur simultaneously in six directions radiating from the centre every 60°. Then the contrast is similar to a distorted hexagon. Sometimes triangles are observed also.

Fig. 6 shows a SEM image of an inclusion sectioned by the surface. The EDX spectrum indicates that the inclusion contains mainly Cd. The diameter of the spot in fig. 6 coincides with the one of the IR contrast.

Fig. 6. SEM photograph of an inclusion cut by the surface (excess Te).

4. Discussion

The IR contrast of Te inclusions arises from complete absorption in a transparent matrix. The same holds for Cd inclusions, but they are surrounded by a not totally absorbing layer achieving a thickness of some diameters. It is assumed that this additional contrast arises from dislocations decorated with atoms of the excess component. Braun and Helberg [10] performed micro hardness indentations on CdTe. They obtained the well-known etch pit rosette on {111} planes consisting of 6 double arms which point in ⟨110⟩ directions. From their analysis the transport of the material parallel to the surface occurs by 60° edge dislocations loops, whereas the material transport into the volume is done by screw dislocations. They form narrow loops in ⟨110⟩ directions. In case of a spherical stress concentration,

material is pressed into the volume in all directions. This stress is released by punching out narrow screw dislocation loops in all ⟨110⟩ directions in the CdTe lattice. A three-dimensional pattern arises, well represented by the Thompson tetrahedron with its edges extended several times above its geometrical dimensions. Nearly all projections of such a Thompson tetrahedron are star shaped. They only differ in the lengths and directions of the ⟨110⟩ lines. However, the ⟨100⟩ projection is a distinctive one. This appears to be a square in outline. Fig. 7 shows projections of the Thompson tetrahedron in ⟨111⟩, ⟨110⟩ and ⟨100⟩ directions with the corresponding IR contrast of the Cd inclusion. The square-shaped IR contrast in ⟨100⟩ direction is good confirmation of our model. In ref. [5], Watson et al. give a misleading description of the composition, but confirm the Cd content of the inclusion [11].

Now the question has to be answered, why Cd inclusions are surrounded by dislocations, in contrast to Te inclusions. Looking at the temperature–composition projection of the CdTe phase diagram [12], one realizes the asymmetric shape of the liquidus curve with respect to the CdTe compound. Up to 600°C the solubility of Te in Cd is extremely low. This means that during the cooling process the final hole in the CdTe matrix for the liquid Cd droplet is already formed at this temperature. The solidification of Cd at 321°C causes a volume misfit between matrix and inclusion. The thermal expansion coefficients of CdTe and Cd are 4.5×10^{-6} and 31×10^{-6} K^{-1}, respectively, giving rise to a further volume misfit.

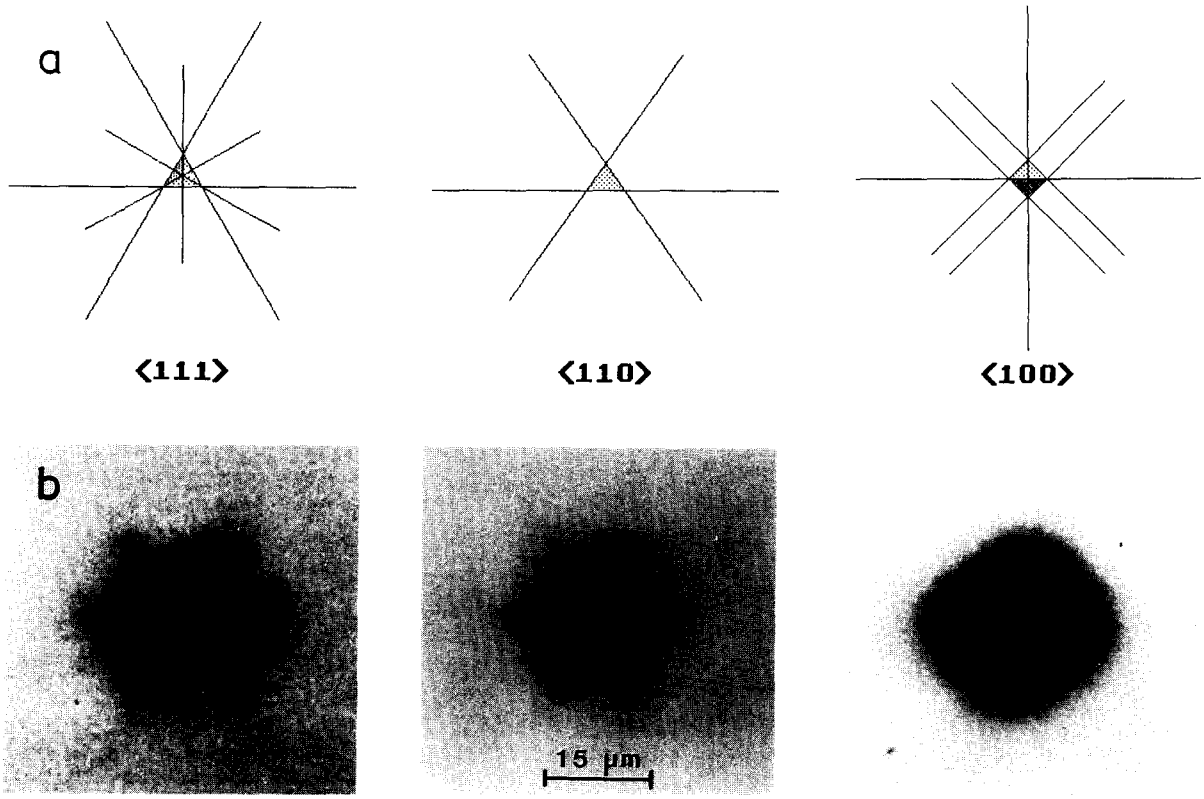

Fig. 7. (a) Thompson tetrahedron in ⟨111⟩, ⟨110⟩ and ⟨100⟩ projections. (b) IR contrast in ⟨111⟩, ⟨110⟩ and ⟨100⟩ projections.

Obviously, these misfit mechanisms result in a larger shrinkage of the inclusion than of the CdTe matrix. Then matrix material is released into the hollow spaces by the same dislocation configuration as described above with opposite sign of the involved Burgers vectors. The Te inclusions reach their equilibrium composition not before their solidification temperature of 450°C. Down to this temperature there is a mass transport between inclusion and matrix. Additionally, the difference in the thermal expansion coefficient of CdTe and Te (14.7×10^{-6} K^{-1}) is less.

5. Conclusion

Cd and Te inclusions in a monocrystalline matrix show a profound difference in the transmission IR image contrast. Cadmium inclusions are surrounded by screw dislocations punched out by stress relief. Thus the IR contrast appears to be 6 times larger in diameter than that of the inclusion. The outline of the IR contrast normally is star-shaped except in the ⟨100⟩ direction. Then it is square-shaped. These features are typical for Cd inclusions. Te inclusions show a circular contrast pattern with a very sharp outline. For bigger inclusions the circular shape may be distorted to a hexagon. The contrast diameter corresponds to the real particle diameter.

Acknowledgements

The authors thank D. Plischke for support with their SEM investigations. The IR microscope was supplied by the Zentrum für Funktionswerkstoffe, Göttingen.

References

[1] D.J. Williams and A.W. Vere, J. Crystal Growth 83 (1987) 341.
[2] K.Y. Lay, D. Nichols, S. McDavitt, B.E. Dean and C. Johnson, J. Crystal Growth 86 (1988) 118.
[3] K. Durose and G.J. Russel, J. Crystal Growth 101 (1990) 246.
[4] J.L. Pautrat and N. Magnea, J. Appl. Phys. 53 (1982) 8668.
[5] C.C.R. Watson, K. Durose, A.J. Banister, E. O'Keefe and S.K. Bains, Mater. Sci. Eng. 16 (1993) 113.
[6] N. Wang and P. Haasen, Phys. Status Solidi (a) 128 (1991) 37.
[7] K. Durose, G.H. Russel and J. Woods, in: Microscopy of Semiconducting Materials 1985, Inst. Phys. Conf. Ser. 76, Eds. A.G. Cullis and D.B. Holt (Inst. Phys., Bristol, 1985) p. 327.
[8] R. Triboulet and Y. Marfaing, J. Electrochem. Soc. 120 (1973) 1260.
[9] K. Kanaya and S. Okayama, J. Appl. Phys. 5 (1972) 42.
[10] C. Braun and H.W. Helberg, Phil. Mag. A 53 (1986) 277.
[11] C.C.R. Watson, private communication.
[12] K. Zanio, in: Semiconductors and Semimetals, Vol. 13 (Academic Press, New York, 1978).